

SIMULATION OF NUCLEAR FUSION  
USING A ONE DIMENSIONAL PARTICLE IN CELL METHOD

By

Steven T. Margell

A Thesis Presented to

The Faculty of Humboldt State University

In Partial Fulfillment of the Requirements for the Degree

Master of Science in Environmental Systems: Mathematical Modeling

Committee Membership

Dr. Ken Owens, Committee Chair

Dr. Monty Mola, Committee Member

Mr. Tim Lauck, Committee Member

Dr. Rick Zechman, Graduate Coordinator

December 2016

## DEDICATION

This work is dedicated to my family.

Most especially to Emilie for supporting me as my wife, partner, and best friend.

Your love is a constant source of inspiration and encouragement.

## ABSTRACT

### SIMULATION OF NUCLEAR FUSION USING A ONE DIMENSIONAL PARTICLE IN CELL METHOD

Steven T. Margell

In this thesis several novel techniques are developed to simulate fusion events in an isotropic, electrostatic three-dimensional Deuterium-Tritium plasma. These techniques allow us to accurately predict three-dimensional collision events with a one-dimensional model while simultaneously reducing compute time via a nearest neighbor algorithm. Further, a fusion model based on first principles is developed that yields an average fusion reactivity which correlates well with empirical results.

## ACKNOWLEDGEMENTS

This work would not have been possible without the support and direction of the thesis committee members, each of which played a crucial role in the development and completion of this project. Primarily, I would like to thank Dr. Kenneth Owens for providing me with guidance throughout this project. Great thanks go to Dr. Monty Mola for educating me in Physics as an undergraduate and providing valuable insight into this project. Thanks to Tim Lauck for his support and developing fundamental concepts related to this project. Many thanks to Dr. Chris Dugaw for his support and encouragement, as well as my colleagues in the Mathematics department.

A special thanks to Dr. Rollin Richmond for his contributions through the Humboldt State University President's Office as well as the Humboldt State University Loyalty Fund towards the construct of the FUSION supercomputer. This project is a testament to the educational benefit of the supercomputer and has only begun to explore the potential of this tool as a teaching and research aid.

Finally, I would like to thank the Department of Mathematics at Humboldt State University for giving me the opportunity to study under their direction.

-Steven Margell

## TABLE OF CONTENTS

DEDICATION . . . . .	ii
ABSTRACT . . . . .	iii
ACKNOWLEDGEMENTS . . . . .	iv
TABLE OF CONTENTS . . . . .	v
LIST OF FIGURES . . . . .	vii
INTRODUCTION . . . . .	1
Synopsis . . . . .	1
Background . . . . .	1
Challenges . . . . .	3
MODEL . . . . .	5
Primary Assumptions . . . . .	5
Nonrelativistic Velocities . . . . .	6
Maxwell-Boltzman Speed Distribution . . . . .	6
Relative Coordinate Frame . . . . .	7
Coulomb Scattering . . . . .	8
One-Dimensional Coulomb Scattering . . . . .	9
Collision Cross Section and Coulomb Logarithm . . . . .	10
Quantum Mechanical Tunneling . . . . .	11
Theoretical Fusion Reactivity . . . . .	15
Fusion Reactivity Computation . . . . .	18
SIMULATION . . . . .	20
1D Particle Simulation . . . . .	20
An Appropriate Timestep . . . . .	21
Particle Interaction Range . . . . .	22
Simulated Three-Dimensional Energy . . . . .	24
Fusion Probability . . . . .	24
RESULTS . . . . .	25
Separation . . . . .	25
Relative Velocity . . . . .	27
Relative Velocity vs. Separation . . . . .	28
Reactivity . . . . .	30

DISCUSSION . . . . .	33
Future Work . . . . .	33
BIBLIOGRAPHY . . . . .	35
APPENDIX . . . . .	36
Constants and Calculations . . . . .	36

## LIST OF FIGURES

Figure		Page
1	The 5-node cluster built in 2009 during a Research Experience for Undergraduates under the direction of Dr. Kenneth Owens. The current one-dimensional plasma simulation is shown to be actively running in parallel across two nodes. . . . .	2
2	An undergraduate student measures CPU temperatures during the construction and benchmarking of the FUSION supercomputer. The thesis author and Dr. Kenneth Owens (far right) supervise. . . . .	3
3	Transforming particle positions from the Laboratory coordinate system to a Relative Frame simplifies calculations and is illustrative of the conservation of momentum between a pair of particles. In the relative frame one particle is fixed and the other particle is moving relative to it at a separation of $\mathbf{r}$ . . .	7
4	Particle Orbit due to a Coulomb potential. A deflection of 90 degrees occurs for a separation where $b = b_o$ . . . . .	9
5	Gamow's model for the potential energy of a tunneling particle and a representative wave function. . . . .	12
6	Average fusion reactivity for Deuterium-Tritium interactions as determined by the Naval Research Laboratory (Huba, 2013). A peak is found at approximately 50-100 keV. For energies lower than this peak there are a higher number of collision events but low probability of fusion for each. For energies higher than this peak the probability of fusion is increasing, but the collision cross section is decreasing more rapidly which results in fewer collisions and consequently fewer fusion events. . . . .	17
7	Separation in meters between fusion pairs at a kinetic temperature of 100 keV. Head-on collisions plotted in black and overtaking collisions plotted in gray. Separation distance is plotted logarithmically. . . . .	26
8	Probability Density of the Separation in meters between fusion pairs at a kinetic temperature of 100 keV. Separation distance is plotted logarithmically. . . . .	26

9	Relative Velocity in meters per second of fusion pairs at a kinetic temperature of 100keV. Head-on collisions plotted in black and overtaking collisions plotted in gray. Relative Velocities are plotted logarithmically. . . . .	27
10	Probability Density of Relative Velocity plotted logarithmically for Fusion pairs at a kinetic temperature of 100 keV. . . . .	28
11	Relative Velocity as a function of Separation plotted logarithmically for Fusion pairs at a kinetic temperature of 100 keV. . . . .	29
12	Simulation and Naval Research Laboratory (Huba, 2013) average fusion reactivity from 6 simulations of 1000 timesteps plotted logarithmically. NRL fusion reactivity values are plotted as red triangles. Simulation fusion reactivity values are plotted as black circles. Error bars represent a 95% confidence interval. . . . .	31



## INTRODUCTION

### Synopsis

In this thesis a one-dimensional model of fusion by quantum tunneling in an isotropic, electrostatic nonrelativistic Deuterium-Tritium plasma is developed. This model is incorporated into an existing Particle-In-Cell (PIC) computer code and run on a supercomputer. The resulting output is scaled to three dimensions with the resulting fusion events per volume compared to theoretical predictions.

### Background

In 2009 I participated in a Research Experience for Undergraduates at Humboldt State University working with Dr. Kenneth Owens to build a computer cluster for parallelizing a one-dimensional PIC code simulating a Deuterium-Tritium plasma. Dr. Owens modified a PIC simulation of electron motion, originally developed by Fitzpatrick (2006), to include ion interactions. We constructed a 5-node cluster (Figure 1) and the simulation was distributed across all nodes using the cluster management software ROCKS. We attempted to incorporate the Message Passing Interface for parallel communications but were unsuccessful.

After the REU Owens continued with the project using the MOSIX Cluster Management System to successfully run the simulation on every central processing unit (CPU) core across the cluster. Though this was a successful proof of concept, the cluster was too small for practical applications. Dr. Owens secured funding from the Humboldt State University Loyalty Fund and the President's Office under Dr. Rollin Richmond and built the FUSION supercomputer in order to use Graphics Processing Units (GPU's) as computation cores. FUSION is capable of 110 teraflops or 110 trillion computations per second.

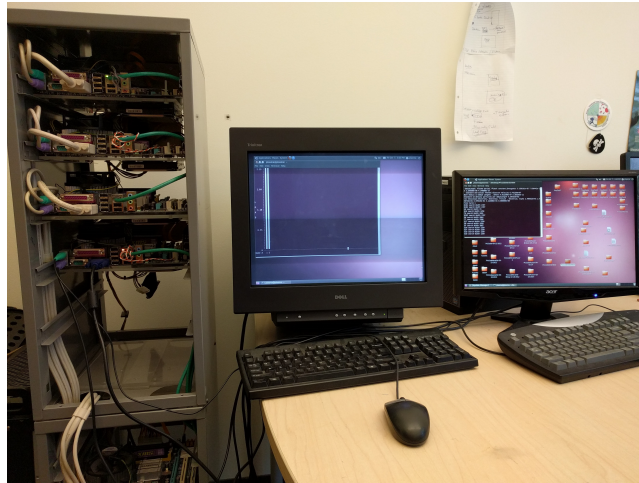


Figure 1: The 5-node cluster built in 2009 during a Research Experience for Undergraduates under the direction of Dr. Kenneth Owens. The current one-dimensional plasma simulation is shown to be actively running in parallel across two nodes.

I returned to the group in 2013 and assisted in the design and construction of FUSION (Figure 2). From the REU until this time, Owens and Lauck (2017) provided critical groundwork for this thesis by developing a simulation that models particle interactions in one dimension which accurately predicts the number of collisions in three dimensions. Owens et al. are planning to write code to utilize the GPU's on FUSION but that project is beyond the scope of this thesis. The plasma fusion simulation developed for this thesis uses CPU cores across the supercomputer.

In this thesis a technique developed by Owens and Lauck (2017) is used to greatly reduce the collision simulation time using a nearest neighbor approach. This technique reduces simulation times from 20 minutes to 8 seconds. Previous simulations checked every particle against every other particle which allowed for accurate collision calculations but was computationally intensive. The nearest neighbor simulations run on a time scale that accurately counts ion collisions. However, since the electrons move much faster than ions, the simulation does not accurately count electron collisions. This limitation should

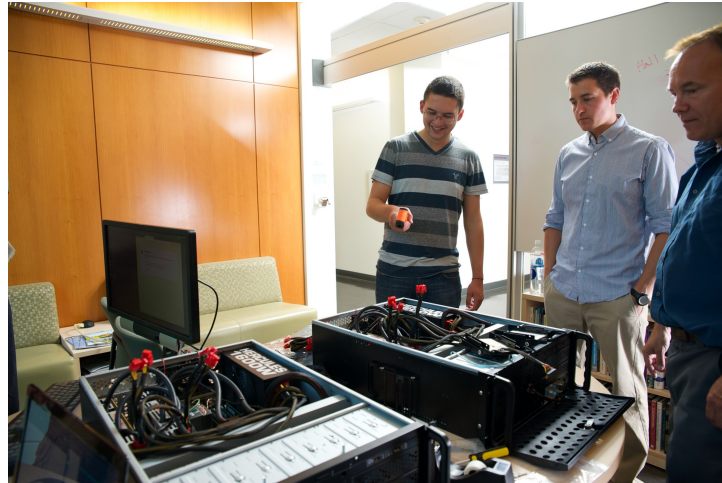


Figure 2: An undergraduate student measures CPU temperatures during the construction and benchmarking of the FUSION supercomputer. The thesis author and Dr. Kenneth Owens (far right) supervise.

not affect this thesis which explores ion collisions.

### Challenges

The current model for quantum tunneling has taken several years to develop and implement, with many challenges and dead-ends encountered along the way. Originally, the fusion model utilized a multiple fusion attempt procedure calculated from the kinetic energy of the particle based on Griffiths (2005) colloquial description of an alpha particle “rattling around” inside a nucleus. This model proved to be unnecessary, non-physical, and was abandoned, being replaced by the model described in this thesis.

The simulated one-dimensional fusion count was originally too low. After running months of fusion simulations across various kinetic energy levels, we realized that the simulation timestep was responsible. A timestep that is too short results in too few fusion events. Similarly, a timestep that is too long results in allowing particles to pass potential collision opportunities resulting in less fusion events than theory predicts. This issue is

addressed in the Simulation section of this thesis.

One-dimensional particles have only a third of the kinetic energy of three-dimensional particles resulting in insufficient energy to overcome Coulomb repulsion and fuse. To solve this problem, two other velocity components are simulated by sampling velocities from other Deuterium-Tritium collision pairs. Combining these components yields an estimated three-dimensional kinetic energy providing sufficient energy for fusion.

## MODEL

### Primary Assumptions

There are three primary assumptions made to simplify calculations. First, the plasma is assumed to be isotropic and in thermal equilibrium. In the future the working group will include non-isotropic conditions in the plasma but for the purpose of this thesis we assume an isotropic plasma. We call this the “Equilibrium Assumption.”

Second, we assume that the one-dimensional particle simulation of Owens and Lauck (2017) correctly predicts three-dimensional collision densities in isotropic plasmas. This approach is novel and is actively being prepared for publication. This technique assumes that the three-dimensional collision density,  $\rho_{3D}$ , can be computed by cubing the one-dimensional collision density,  $\rho_{1D}$ , according to

$$\rho_{3D} = \rho_{1D}^3. \tag{1}$$

This assumption will be referred to as the “Collision Density Assumption” and is used in this thesis to scale the one-dimensional simulation collision frequencies to three dimensions.

Finally, we assume that all particle collisions are elastic, unless fusion occurs, and that all particle velocities are nonrelativistic, following a Maxwell-Boltzman distribution. This ensures that Newton’s laws of mechanics are valid and simplifies calculations (Thornton and Rex, 2006). We call this the “Nonrelativistic Assumption.”

### Nonrelativistic Velocities

Particles traveling at nonrelativistic velocities can be described with Newtonian mechanics and do not require relativistic transformations. To determine whether particle velocities are relativistic, we must consider the Lorentz factor,  $\gamma$ ,

$$\gamma = \frac{1}{\sqrt{1 - \frac{v^2}{c^2}}}, \quad (2)$$

where  $v$  is the velocity of the ions and  $c$  is the speed of light.

If  $\gamma \approx 1$  Newton's laws of mechanics are valid (Thornton and Rex, 2006). The largest relative velocity will yield the greatest value for  $\gamma$ . For the largest recorded relative ion velocity in the simulation,  $1.75 \times 10^7 \frac{m}{s}$ , the corresponding value of  $\gamma$  is 1.00199. The calculation can be found in the Appendix Mathematica attachment. The resulting value of  $\gamma$  verifies that particle interactions can be treated nonrelativistically and calculated using Newtonian Physics.

### Maxwell-Boltzman Speed Distribution

In an ideal gas, particle speeds follow a Maxwell-Boltzman distribution (Serway et al., 2005). To ensure that it is appropriate for the simulation to initialize particle speeds according to this distribution, the average one-dimensional inter-particle spacing,  $\eta_{1D}^{-1}$ , must be greater than the thermal deBroglie wavelength,  $\lambda_{th}$  (Schroeder, 2000):

$$\lambda_{th} \ll \eta_{1D}^{-1} \quad \text{where} \quad \lambda_{th} = \frac{2\pi\hbar}{\sqrt{2\pi mkT}}. \quad (3)$$

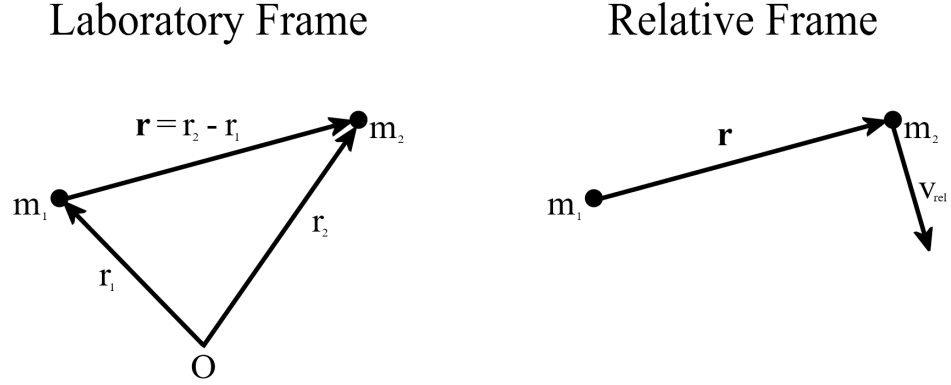


Figure 3: Transforming particle positions from the Laboratory coordinate system to a Relative Frame simplifies calculations and is illustrative of the conservation of momentum between a pair of particles. In the relative frame one particle is fixed and the other particle is moving relative to it at a separation of  $\mathbf{r}$ .

$\hbar$  is Planck's constant,  $k$  is the Boltzmann constant,  $T$  is the temperature of the gas, and  $m$  is the mass of the particle of interest (or reduced mass,  $\mu$  for two particles).

The deBroglie wavelength,  $\lambda_{th}$ , varies from  $4.3 \times 10^{-12}$  meters for an electron to  $9.2 \times 10^{-14}$  meters for the Deuterium-Tritium pair. The one-dimensional density of the plasma is four times the ion density per species since there are two ion species, Deuterium and Tritium, and each ion has an associated electron. The simulations in this thesis have a inter-particle spacing of  $2.7 \times 10^{-10}$  meters which is two orders of magnitude greater than the largest  $\lambda_{th}$  of any particles in the plasma (see the Appendix Mathematica attachment for calculations). So, it is appropriate to use a Maxwell-Boltzman distribution for each species.

### Relative Coordinate Frame

Particle collisions are well described by a generalized coordinate system which describes the motion of the center of mass and the motion of one particle relative to the other (Taylor, 2005). In this relative coordinate frame one particle is fixed and the other particle is moving

relative to it at the relative position  $\mathbf{r}$  (see Figure 3). In this relative frame the equation of motion of one particle relative to the other becomes

$$\mu \ddot{\mathbf{r}} = -\nabla U(r), \quad (4)$$

where  $\mu = \frac{m_1 m_2}{m_1 + m_2}$  is the reduced mass for two particles of mass  $m_1$  and  $m_2$  respectively,  $\mathbf{r}$  is the relative position and  $r = |\mathbf{r}|$  is the separation between the particles.  $U(r)$  is the Coulomb potential energy given by

$$U(r) = \frac{q_1 q_2}{4\pi\epsilon_o r}, \quad (5)$$

where  $q_1$  and  $q_2$  are the respective charge of the two particles and  $\epsilon_o$  is the permittivity of free space. Most calculations in this thesis are performed in the relative frame with the potential energy between the two particles described by Coulomb repulsion (Equation 5).

### Coulomb Scattering

Particle interactions, such as collision or fusion events, are determined from the magnitude of the separation between the particles and modeled using Coulomb scattering theory. Goldston and Rutherford (2000) explain that every three-dimensional collision can be described in a two-dimensional plane using relative coordinates. If there were no Coulomb force between two particles, the distance of closest approach in a plane is  $b$ , called the impact parameter (see Figure 4). However, between ions there exists a Coulomb repulsion and the scattering angle,  $\theta$ , is a function of the impact parameter,  $b$ , where

$$b = b_o \sqrt{\frac{1 + \cos \theta}{1 - \cos \theta}} \quad \text{and} \quad b_o = \frac{q_1 q_2}{4\pi\epsilon_o \mu v_{rel}^2}. \quad (6)$$



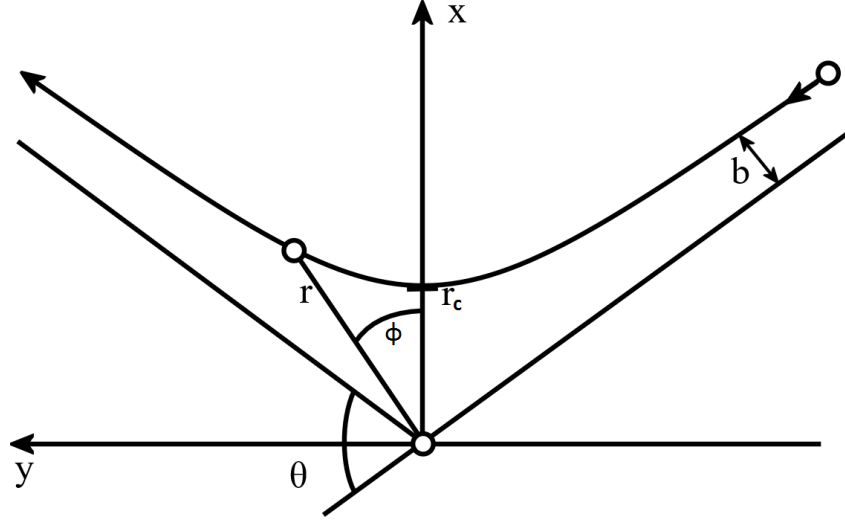


Figure 4: Particle Orbit due to a Coulomb potential. A deflection of 90 degrees occurs for a separation where  $b = b_o$ .

It can be seen that  $b_o$  is the impact parameter that corresponds to 90 degree deflections and is defined in terms of the reduced mass,  $\mu$ , and relative velocity,  $v_{rel} = |\mathbf{v}_2 - \mathbf{v}_1|$ . The classical orbit, in two-body Coulomb scattering, is given by the hyperbolic curve defined by Thornton and Rex (2006) as

$$r = \frac{r_o}{1 - \alpha \cos \phi} \quad \text{where} \quad r_o = \frac{b^2}{b_o} \quad \text{and} \quad \alpha = \sqrt{1 + \left(\frac{b}{b_o}\right)^2}. \quad (7)$$

### One-Dimensional Coulomb Scattering

The Coulomb scattering in a plane is transformed to a one-dimensional model where the closest approach,  $r_c$ , is the separation distance where the kinetic energy of the reduced mass particle is equal to the potential energy due to Coulomb repulsion,

$$\frac{1}{2} \mu v_{rel}^2 = \frac{q_1 q_2}{4\pi \epsilon_o r_c}. \quad (8)$$

Solving for the closest approach we find that

$$r_c = \frac{2q_1q_2}{4\pi\epsilon_o\mu v_{rel}^2}, \quad \text{so} \quad r_c = 2b_o^{1D}, \quad (9)$$

where  $b_o^{1D}$  is calculated by substituting the one-dimensional relative velocity into Equation 6. In the simulation, particles are checked at a given timestep to see if they have been moved by the background electric field within a separation of  $2b_o^{1D}$ . If they are within this distance and their relative velocity is moving them towards one another, then the model collides the particles and evaluates them for a fusion event.

### Collision Cross Section and Coulomb Logarithm

A particle traveling into a gas has a collision cross section,  $\sigma$ , which is an area that measures the likelihood a particle will collide with another particle. The 90 degree or more scattering cross section, developed by Goldston and Rutherford (2000), can be written in the relative frame as

$$\sigma_{90+} = \frac{Z^2 e^4}{16\pi\epsilon_o^2 \mu^2 v_{rel}^4} \quad (10)$$

for particles with atomic number  $Z$ , mass  $\mu$ , and velocity of  $v_{rel}$ . It is important to notice that higher energy particles have a collision smaller cross section allowing a particle to travel further into a volume of gas before colliding.

In a three-dimensional plasma multiple small-angle collisions can aggregate to cause a deflection of 90 degrees or greater. Goldston and Rutherford (2000) showed that the Coulomb logarithm,  $\ln \Lambda$ , can be used to account for this effect. The Coulomb logarithm is defined as

$$\ln \Lambda = \ln \left( \frac{\lambda_D}{b_o} \right) \quad \text{where} \quad \lambda_D = \sqrt{\frac{\epsilon_o T_e}{\eta_e e^2}}. \quad (11)$$

The Debye length,  $\lambda_D$ , measures how far the electrostatic effects of a charged particle persist. Beyond this distance a particle's charge is shielded by the electrostatic field. The Debye length depends on the electron temperature,  $T_e$ , the electron density,  $\eta_e$ , and the elementary charge,  $e$ . Goldston and Rutherford (2000) showed that

$$b_o \approx \frac{Z}{12\pi\eta_{3D}\lambda_D^2} \quad (12)$$

where  $Z$  is the atomic number of the ion species of interest and  $\eta_{3D}$  is the three-dimensional ion density. So, the Coulomb logarithm can be approximated as

$$\ln \Lambda \approx \ln \left( \frac{12\pi\eta_{3D}\lambda_D^3}{Z} \right). \quad (13)$$

To compute the total collision cross section, which accounts for multiple small angle collisions that aggregate to a 90 degree or more scattering, Goldston and Rutherford (2000) showed that this total collision cross section,  $\sigma$ , can be approximated as

$$\sigma = \frac{Z^2 e^4 \ln \Lambda}{4\pi\epsilon_o^2 \mu^2 v_{rel}^4}. \quad (14)$$

From Equations 10 and 14, it can be seen that this total collision cross section is a factor of  $4 \ln \Lambda$  greater than  $\sigma_{90+}$ . Thus, the total collision count in a volume is the number of 90 degree or greater scattering events multiplied by  $4 \ln \Lambda$ .

### Quantum Mechanical Tunneling

Due to quantum mechanical tunneling, every colliding pair of Deuterium and Tritium ions has a probability of fusing. Fusion occurs when one particle “tunnels” through the Coulomb

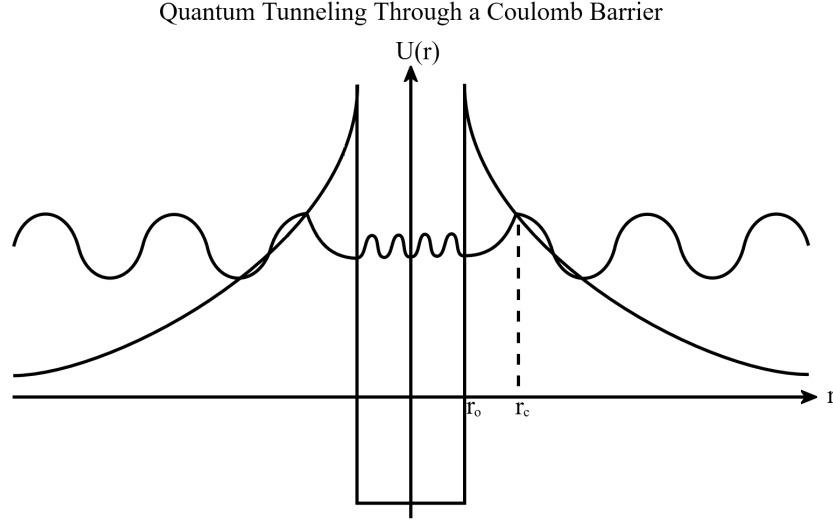


Figure 5: Gamow's model for the potential energy of a tunneling particle and a representative wave function.

barrier of the other. The tunneling model used in this thesis is built on Gamow (1928) as presented by Griffiths (2005). The potential energy in this model for distances less than the nuclear radius,  $r_o$ , is a square well where the particles will fuse together, see Figure 5. For distances greater than the nuclear radius there is a Coulomb repulsion between the two particles.

For a particle of reduced mass  $\mu$  and relative energy  $E$  traveling through a region of space where there is a potential  $U(r)$ , the time independent Schrödinger equation for a wavefunction,  $\Psi(r)$ , is

$$-\frac{\hbar^2}{2\mu} \frac{d^2\Psi(r)}{dr^2} + U(r)\Psi(r) = E\Psi(r). \quad (15)$$

This can be rewritten as

$$\frac{d^2\Psi(r)}{dr^2} = -\frac{p(r)^2}{\hbar^2}\Psi(r) \quad \text{where} \quad p(r) = \sqrt{2\mu[E - U(r)]}, \quad (16)$$

and  $p(r)$  is the classical momentum. Using the WKB approximation, Griffiths (2005) shows the solution to the wave equation is

$$\Psi(r) = \frac{C}{\sqrt{p(r)}} e^{\pm i \int p(r) dr / \hbar}, \quad (17)$$

where  $i$  is the imaginary unit.

Conservation of energy implies that in the relative coordinate frame

$$\frac{p^2}{2\mu} + \frac{e^2}{4\pi\epsilon_o r} = E, \quad (18)$$

so the momentum can be written as

$$p(r) = \sqrt{2\mu \left( E - \frac{e^2}{4\pi\epsilon_o r} \right)}. \quad (19)$$

However, the relative energy of the particle is less than the potential energy for  $r_o < r < r_c$  and the momentum will be imaginary,

$$p(r) = i \sqrt{2\mu \left( \frac{e^2}{4\pi\epsilon_o r} - E \right)}. \quad (20)$$

This results in an additional factor of  $i$  in the solution to the wave equation which implies the general solution

$$\Psi(r) = \frac{C}{\sqrt{|p(r)|}} e^{\pm \int |p(r)| dr / \hbar}. \quad (21)$$

Griffiths (2005) uses Equation 21 to describe the probability of a particle tunneling

through the potential barrier between  $r_o < r < r_c$  as

$$T \cong e^{-2\gamma} \quad \text{where} \quad \gamma = \frac{1}{\hbar} \int_{r_o}^{r_c} |p(r)| dr. \quad (22)$$

Since one-dimensional collisions in the relative frame are head-on, at the instant of the collision all kinetic energy has transformed into potential energy, so

$$E = \frac{e^2}{4\pi\epsilon_o r_c} \quad (23)$$

where  $r_c$  is the closest approach. From this we solve for the closest approach,

$$r_c = \frac{e^2}{4\pi\epsilon_o E}. \quad (24)$$

Now,  $\gamma$  can be computed by substituting the momentum from Equation 20 into 22,

$$\begin{aligned} \gamma &= \frac{1}{\hbar} \int_{r_o}^{r_c} \sqrt{2\mu \left( \frac{e^2}{4\pi\epsilon_o r} - E \right)} dr \\ &= \frac{\sqrt{2\mu E}}{\hbar} \int_{r_o}^{r_c} \sqrt{\frac{r_c}{r} - 1} dr. \end{aligned} \quad (25)$$

Integrating by making the substitution  $r = r_c \sin^2 u$  and using the simplifying assumption that  $r_o \ll r_c$ , this can be rewritten as

$$\begin{aligned} \gamma &= \frac{\sqrt{2\mu E}}{\hbar} \left[ \frac{\pi}{2} r_c - 2\sqrt{r_o r_c} \right], \\ &= \frac{\sqrt{2\mu}}{\hbar} \frac{\pi}{2} \frac{e^2}{4\pi\epsilon_o} \frac{1}{\sqrt{E}} - \frac{2\sqrt{2\mu}}{\hbar} \left( \frac{e^2}{4\pi\epsilon_o} \right)^{1/2} \sqrt{r_o}. \end{aligned} \quad (26)$$

We define the constants

$$E_o = \left[ \left( \frac{e^2}{4\pi\epsilon_o} \right) \frac{\pi}{2} \frac{\sqrt{2\mu}}{\hbar} \right]^2 \quad \text{and} \quad R_o = \left[ \left( \frac{e^2}{4\pi\epsilon_o} \right)^{\frac{1}{2}} 2 \frac{\sqrt{2\mu}}{\hbar} \right]^{-2}, \quad (27)$$

resulting in a simplified expression for  $\gamma$ :

$$\gamma = \sqrt{\frac{E_o}{E}} - \sqrt{\frac{r_o}{R_o}}. \quad (28)$$

To compute the tunneling probability, the energy  $E$  is taken to be the initial relative kinetic energy before particle interactions begin since the potential energy at infinity is zero. For numerical values of  $E_o$ ,  $R_o$ , and the nuclear radius  $r_o$  see the Appendix Mathematica attachment.

### Theoretical Fusion Reactivity

The average fusion reactivity is defined as the average reactive volume per second that a particle generates when entering a gas. This reactive volume per second is the product of the particle's fusion cross section and velocity, where the fusion cross section is an area measuring the likelihood that a particle will fuse with another particle. Any particle in this volume will react with the incoming particle. The average reactivity is defined as  $\langle \sigma v \rangle$  where  $\sigma$  is the fusion cross section,  $v$  is the velocity, and the brackets represent averaging over the velocity distribution.

Atzeni and Meyer-Ter-Vehn (2004) showed that in a plasma the volumetric fusion reaction rate,  $R_{ij}$ , for species  $i$  and  $j$  is related to the average fusion reactivity by

$$R_{ij} = \frac{\eta_i \eta_j}{1 + \delta_{ij}} \langle \sigma v \rangle, \quad (29)$$

where  $\eta_i$  and  $\eta_j$  are the densities of the two particle species and  $\delta_{ij}$  is the Kronecker delta function.  $\delta_{ij} = 1$  if  $i = j$  resulting in a factor of 2 in the denominator and  $\delta_{ij} = 0$  if  $i \neq j$  yielding a factor of 1. When a same-species interaction occurs, such as when Deuterium collides with Deuterium, a factor of 2 results from the Kronecker delta function, ensuring that double counting does not occur. In the simulated plasma, the Deuterium-Tritium interactions are of greatest interest and in this case the Kronecker delta function is zero.

From Equation 29, we find the average fusion reactivity,  $\langle \sigma v \rangle$ , in the simulated Deuterium-Tritium model,

$$\langle \sigma v \rangle = \frac{R_{DT}}{\eta_D \eta_T}. \quad (30)$$

Since the density of Deuterium and Tritium are equal, so  $\eta_D = \eta_T = \eta$  and therefore

$$\langle \sigma v \rangle = \frac{R_{DT}}{\eta^2}. \quad (31)$$

Thus, the average fusion reactivity is the number of fusion events per unit time and per unit volume divided by the product of the particle densities. For a simulated cloud of Deuterium ions interacting with a cloud of Tritium ions, it follows that the average number of fusion events per volume in a timestep is

$$R_{DT} \Delta t = \langle \sigma v \rangle \eta^2 \Delta t \quad (32)$$

The Naval Research Laboratory Plasma Formulary (Huba, 2013) provides a table of average experimental fusion reactivity plotted in Figure 6. This curve is the result of fitting experimental results by Duane (1972) and has a peak because the probability of fusion increases with energy while the probability of collision becomes less likely. The peak is at



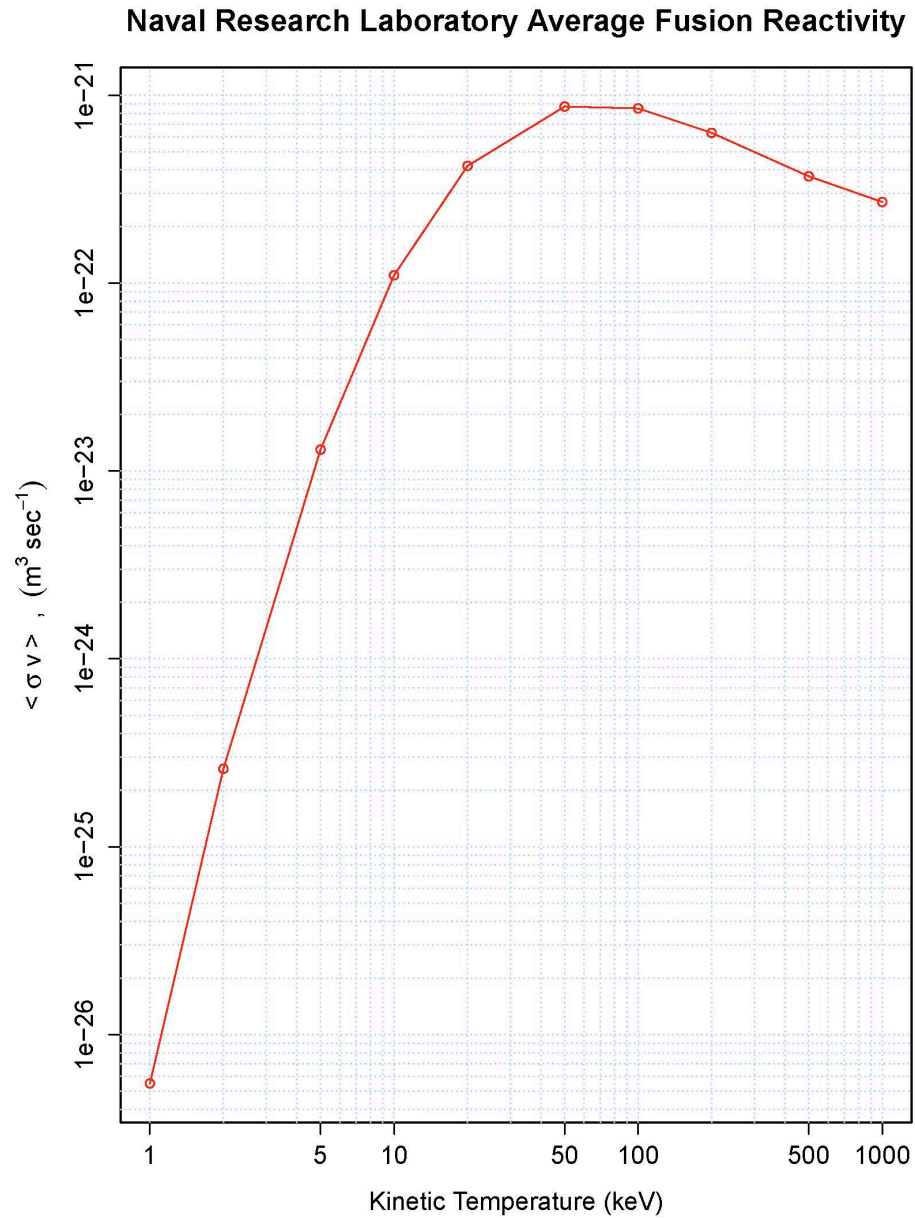


Figure 6: Average fusion reactivity for Deuterium-Tritium interactions as determined by the Naval Research Laboratory (Huba, 2013). A peak is found at approximately 50-100 keV. For energies lower than this peak there are a higher number of collision events but low probability of fusion for each. For energies higher than this peak the probability of fusion is increasing, but the collision cross section is decreasing more rapidly which results in fewer collisions and consequently fewer fusion events.

approximately 50-100 keV.

As energy increases the tunneling probability increases while the collision cross section decreases creating a peak in the average fusion reactivity. The decrease in collision cross section allows for a particle to “slip past” other particles. With fewer collisions at higher energies, there are less opportunities for quantum tunneling and particle fusion.

### Fusion Reactivity Computation

The fusion reactivity is calculated from the count of simulated one-dimensional fusion events as follows. First, the conditional probability of fusion,  $P_F$ , is calculated from the one-dimensional fusion count,  $F_{1D}$ , divided by the one-dimensional collision count,  $C_{1D}$ ,

$$P_F = \frac{F_{1D}}{C_{1D}}. \quad (33)$$

Because three-dimensional velocities are simulated to compute fusion events in the one-dimensional model, Equation 33 yields the correct three-dimensional conditional fusion probability.

Applying the Collision Density Assumption and multiplying by the Coulomb logarithm,  $4 \ln \Lambda$  (Equation 13), we find the predicted collision count,  $C_{3D}$ , per volume,

$$\frac{C_{3D}}{(L\lambda_D)^3} = 4 \ln \Lambda \left( \frac{C_{1D}}{L\lambda_D} \right)^3 \quad (34)$$

The product of the conditional probability of fusion with the collision events per volume yields the predicted three-dimensional fusion count,  $F_{3D}$ , per volume

$$\frac{F_{3D}}{(L\lambda_D)^3} = P_F \frac{C_{3D}}{(L\lambda_D)^3} = 4 \ln \Lambda P_F \left( \frac{C_{1D}}{L\lambda_D} \right)^3. \quad (35)$$

From Equations 32 and 35, the average number of fusion events per volume in a timestep is given by

$$< \sigma v > \eta^2 \Delta t = 4 \ln \Lambda P_F \left( \frac{C_{1D}}{L \lambda_D} \right)^3, \quad (36)$$

and the computed three-dimensional average fusion reactivity is found to be

$$< \sigma v > = \frac{4 \ln \Lambda P_F \left( \frac{C_{1D}}{L \lambda_D} \right)^3}{\eta^2 \Delta t}. \quad (37)$$

## SIMULATION

### 1D Particle Simulation

Fitzpatrick (2006) created computer code to simulate electron interactions in a one-dimensional plasma. This code was expanded upon at Humboldt State University by Owens and Lauck (2017) to include ion motion and collision interactions. The code developed by Owens et al. is a one-dimensional Particle-In-Cell simulation that is capable of accurately modeling isotropic, electrostatic three-dimensional plasma behavior.

The simulation initializes particle positions uniformly across the plasma length with speeds assigned from a Maxwell-Boltzman distribution as described previously. In order to determine the position and velocity of each particle after a defined timestep,  $\Delta t$ , the following occurs: First, the charge density is calculated on an evenly spaced grid spanning the plasma. Second, Poisson's equation is then solved numerically by a Fourier transform to determine the instantaneous electric potential in order to find the electric field. Finally, a fourth-order Runge Kutta method is used to solve for the new position and velocity of each particle.

The simulation identifies a collision event between two particles if the separation between them is less than the closest approach (Equation 9), and their relative velocity puts them on a collision course. After finding a Deuterium-Tritium collision pair, the simulation calculates their tunneling probability which is compared to a uniform random number to determine if fusion has occurred. When a fusion event occurs, both particles are removed from the simulation and replaced by an alpha particle (Helium-4).

The one-dimensional simulation length,  $L\lambda_D$ , is defined in terms of the Debye length,  $\lambda_D$ , and  $L$ , which is a unitless scalar chosen to define the length of the plasma simulated. In this thesis  $N$  particles per species are used with atomic number  $Z = 1$  for Deuterium

and Tritium. Thus, for Deuterium and Tritium ions, the three-dimensional density is

$$\eta_{3D} = \left( \frac{N}{L\lambda_D} \right)^3 \quad (38)$$

and the Coulomb logarithm (Equation 13) becomes

$$\ln \Lambda \approx \ln \left( 12\pi \left( \frac{N}{L} \right)^3 \right). \quad (39)$$

In this thesis there are  $N = 500,000$  particles per ion species and  $L = 10$ , yielding a Coulomb logarithm of

$$\ln \Lambda \approx \ln \left( 12\pi \left( \frac{500,000}{10} \right)^3 \right) = 36.$$

In order to account for small-angle collisions in a three-dimensional plasma, Goldston and Rutherford (2000) showed that the 90 degree or more collision count must be multiplied by a factor of  $4 \ln \Lambda$ . For all simulations in this thesis,  $4 \ln \Lambda = 144$ .

### An Appropriate Timestep

Choosing an appropriate timestep is critical so that collision events are accurately counted. The number of potential collisions in a timestep,  $\Delta t$ , is approximated by  $v_{rel}^{rms} \eta_{1D} \Delta t$  where  $v_{rel}^{rms}$  is the root mean square relative velocity for the Deuterium-Tritium species pair and  $\eta_{1D}$  is the one-dimensional ion density. To estimate  $\Delta t$  so that on average an ion will have approximately one collision per timestep we require

$$v_{rel}^{rms} \eta_{1D} \Delta t \leq 1 \quad \text{and solving for } \Delta t, \quad \Delta t \leq \frac{1}{v_{rel}^{rms} \eta_{1D}}. \quad (40)$$

This choice of the timestep implies that the average particle spacing is

$$v_{rel}^{rms} \Delta t = \frac{1}{\eta_{1D}}. \quad (41)$$

Having an average ion collision frequency of one or less collisions per timestep increases the accuracy of the simulation and greatly reduces the number of particles that must be checked for a collision as described in the following section. The timestep defined in this manner is too large to accurately count electron collision events. This issue will be addressed by the working group in the future and is beyond the scope of this thesis.

One of the advantages of a one-dimensional simulation is that longer time steps may be used. For a three-dimensional plasma the density would yield a much smaller timestep due to the higher number of potential collision pairs. For example, the one-dimensional and the three-dimensional timesteps calculated in the Appendix for 1000 Deuterium and Tritium ions are  $\Delta t_{1D} = 3.29 \times 10^{-14}$  seconds and  $\Delta t_{3D} = 3.29 \times 10^{-20}$  seconds. It would take one million  $\Delta t_{3D}$  timesteps to simulate the same time evolution as a single  $\Delta t_{1D}$  timestep. At 8 seconds per timecycle this would take 92 days.

In this thesis simulations use 500,000 particles across 10 Debye lengths. If the same computer is used, the equivalent  $\Delta t_{3D}$  would take over 700 million years to calculate the time evolution equivalent to a single timestep,  $\Delta t_{1D}$ , used in the simulations.

### Particle Interaction Range

In this thesis all collision pairs are found by considering nearest neighbors within an interaction range,  $R$ . The interaction range is the number of particles checked to either side of each particle to find potential collision pairs.

Every particle is ordered by position into a species specific list. Then the six nearest

neighboring particles on both sides of the particle are checked for a collision; the separation must be within  $2b_o^{1D}$  (Equation 9) and their relative velocity must put them on a collision course. If both criteria are met, then the particles are saved as a collision pair. Then, the next nearest particle is checked in the same fashion.

An appropriate interaction range,  $R$ , will ensure a high likelihood of counting every collision event. This interaction range depends on the standard deviation,  $sd_{rel}$ ,

$$sd_{rel} = \sqrt{\langle v_{rel}^2 \rangle - \langle v_{rel} \rangle^2}, \quad (42)$$

where  $\langle v_{rel}^2 \rangle$  is the average square of the relative velocity and  $\langle v_{rel} \rangle^2$  is the square of the average relative velocity. However, due to the Maxwell-Boltzman distribution of velocities, the one-dimensional average relative velocity will be zero, so

$$sd_{rel} = \sqrt{\langle v_{rel}^2 \rangle} \quad \text{which is} \quad sd_{rel} = v_{rel}^{rms}. \quad (43)$$

The timestep,  $\Delta t$ , found in the preceding section, is defined so that an ion traveling at  $v_{rel}^{rms}$  will cover a distance of one inter-particle separation in a timestep. A particle traveling at six times  $v_{rel}^{rms}$  will cover six inter-particle spacings. Setting  $R = 6$  captures all collision pairs with relative velocities within approximately  $\pm 6$  standard deviations of the mean. This results in a very high probability of detecting all collisions.

Using the particle interaction range greatly reduces the time it takes for a simulation to run. The original number of calculations per timestep was on the order of  $N^2$  for  $N$  ions, but the particle interaction range reduces the calculations to order of  $12N$ . Simulation runtimes are reduced from roughly 20 minutes to 8 seconds per timestep.

### Simulated Three-Dimensional Energy

The tunneling probability of every pair of particles is calculated using a simulated three-dimensional kinetic energy. The kinetic energy for a three-dimensional collision between two particles is calculated using the reduced mass,  $\mu$ , and the relative velocity,  $v_{rel}$ , of each component,

$$K = \frac{1}{2}\mu(v_{relX}^2 + v_{relY}^2 + v_{relZ}^2). \quad (44)$$

The one-dimensional particles have a velocity in only one component direction. To approximate a three-dimensional kinetic energy, we obtain the other two components by sampling the relative velocity from other colliding pairs of Deuterium-Tritium particles. From this, the kinetic energy of a three-dimensional collision is estimated and used to compute a conditional tunneling probability.

### Fusion Probability

Once a Deuterium-Tritium collision pair is found, the fusion probability for that pair is computed from Equation 22. For every collision pair a pseudo uniform random number between zero and one is generated from the rand function in C++. If the fusion probability is greater than this number the pair of particles fuse and are replaced by an alpha particle (Helium-5).



## RESULTS

In this section we will present the results regarding fusing Deuterium-Tritium particle pairs. In particular, their separation distance, velocity distributions, and the average reactive volume per second, called the reactivity, will be shown.

### Separation

The separation distance between fusion pairs for a 1000 timestep simulation at a kinetic temperature of 100 keV is shown in Figure 7. These results are from 500,000 particles per ion species across  $10\lambda_D$ , which is  $5.35 \times 10^{-4}$  meters, and each simulation timestep,  $\Delta t$ , as determined in the Simulation section of this thesis, is  $7.94 \times 10^{-13}$  seconds (see Appendix).

We found a bi-modal distribution illustrated in Figure 7. A distinct grouping of fusing pairs at a separation of approximately  $1 \times 10^{-14}$  meters and another separated by approximately  $5 \times 10^{-11}$  meters. Figure 7 relates the fusion event number, which is simply an index of fusion pairs, to their separation in meters. The particle direction is indicated with black representing head-on collisions and gray representing particles moving in the same direction but with very different velocities so that one particle can overtake the other.

To further explore the particle separation, we consider the probability distribution of the separations in Figure 8. Recall that the nuclear radius,  $r_o$ , is on the order of  $10^{-15}$  meters. Notice, in Figure 8, most separations are greater than this distance. There are no checks written in the simulation PIC code to check for separation distances less than the nuclear radius. Only collision events and motion due to the background electric field keep particles from occupying the same space.

The separation between the particles is related to their relative velocity and to explore

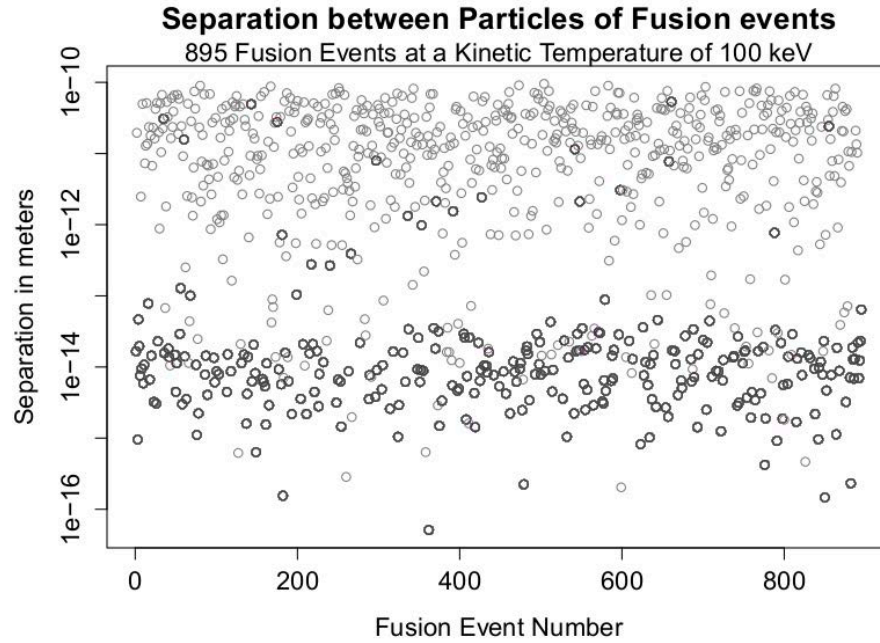


Figure 7: Separation in meters between fusion pairs at a kinetic temperature of 100 keV. Head-on collisions plotted in black and overtaking collisions plotted in gray. Separation distance is plotted logarithmically.

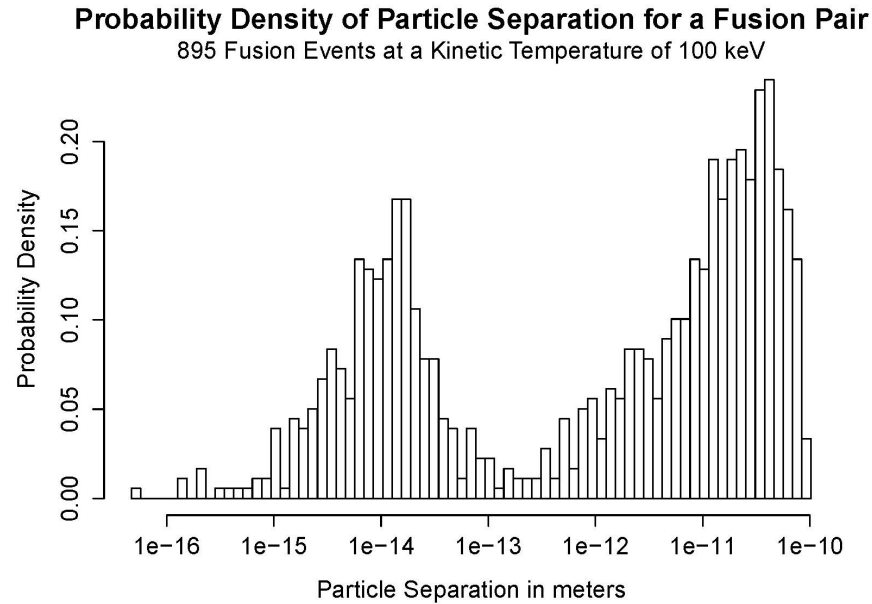


Figure 8: Probability Density of the Separation in meters between fusion pairs at a kinetic temperature of 100 keV. Separation distance is plotted logarithmically.

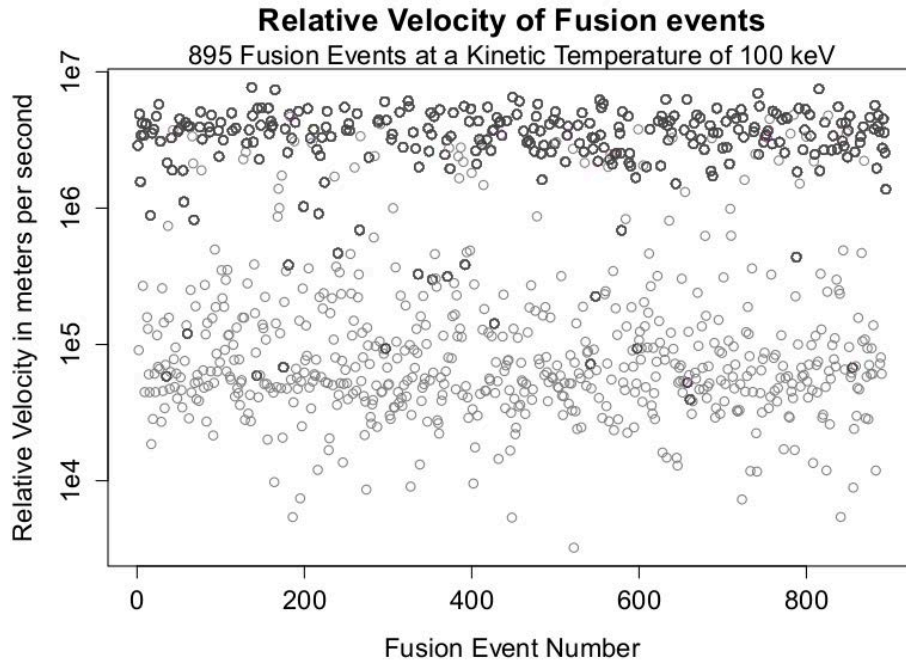


Figure 9: Relative Velocity in meters per second of fusion pairs at a kinetic temperature of 100keV. Head-on collisions plotted in black and overtaking collisions plotted in gray. Relative Velocities are plotted logarithmically.

this structure we examined the relative velocities of the fusing particles.

### Relative Velocity

Similarly to the separation of fusion events, in Figure 9 we see a bi-modal distribution in the relative velocity between fusing particles. Collision events that are head-on are plotted in black and occur when particles are moving in opposite directions (towards one another). Alternatively, particle pairs plotted in gray represent when a high speed particle overtakes a slower particle traveling in the same direction. We determined which of these cases applied by looking at the product of the particles velocities in the laboratory frame, if the product was positive, particles were moving in the same direction, and if the product was negative they were moving in opposite directions.

Next, consider the probability density of the relative velocity in Figure 10. The peak in

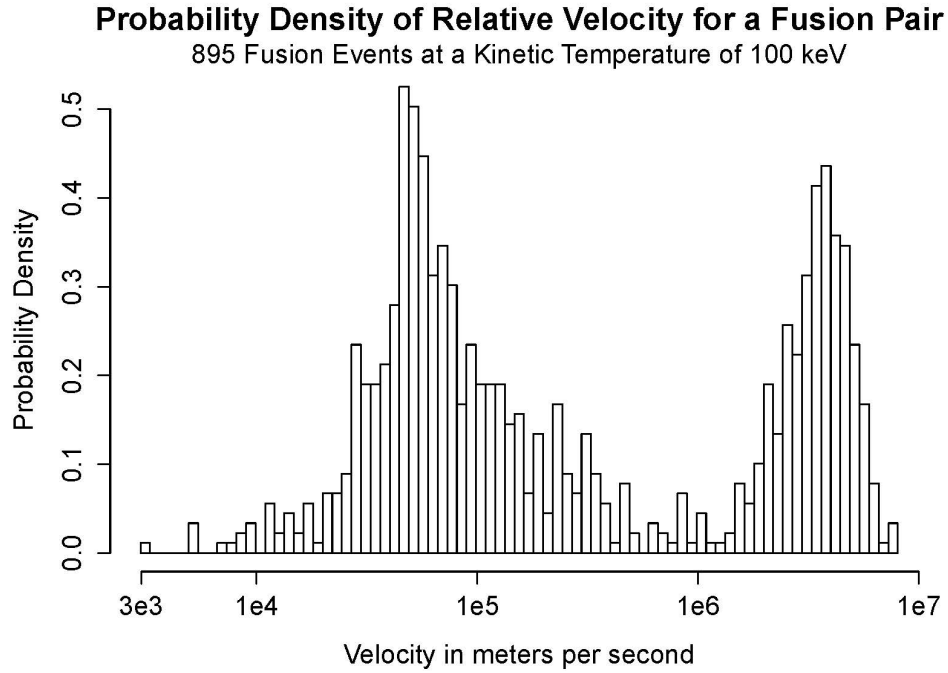


Figure 10: Probability Density of Relative Velocity plotted logarithmically for Fusion pairs at a kinetic temperature of 100 keV.

relative velocity at approximately  $5 \times 10^4$  meters per second is mostly composed of particles that are overtaking one another. The relative velocity peak at approximately  $5 \times 10^6$  meters per second relates almost entirely to head-on collision pairs. There are distinctly fewer fusion pairs at higher velocities due to the collision cross section being smaller for higher energy particles.

#### Relative Velocity vs. Separation

The relationship between the relative velocity and separation,  $r$ , of fusion pairs is shown in Figure 11. There are two distinct lines that separate where fusion events can and cannot occur. The lower line has a positive slope and is expected from the simulation code because

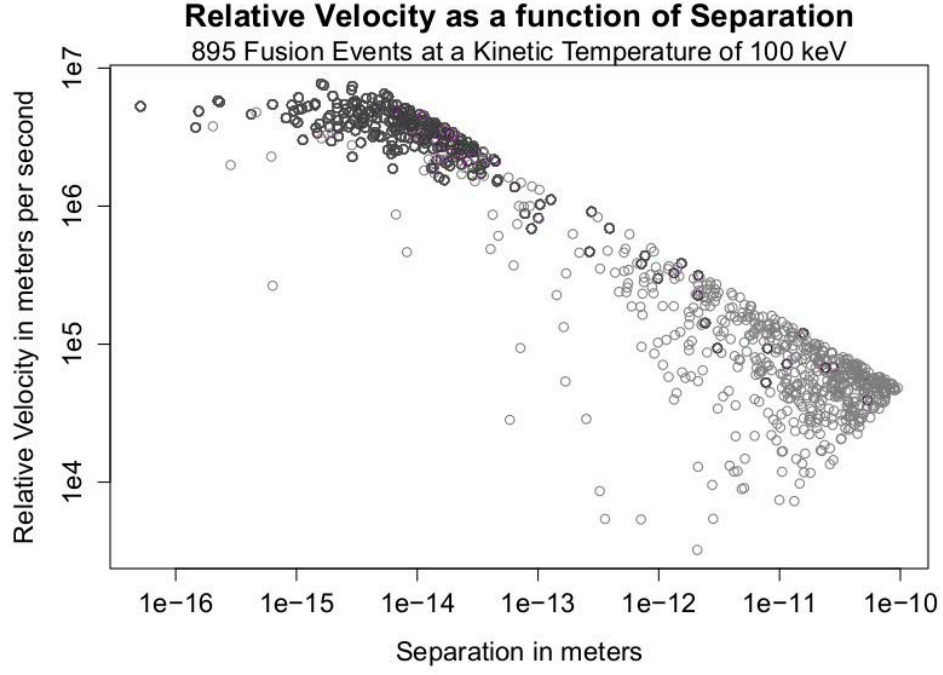


Figure 11: Relative Velocity as a function of Separation plotted logarithmically for Fusion pairs at a kinetic temperature of 100 keV.

every colliding pair of particles must satisfy

$$v_{rel}\Delta t \geq r, \quad (45)$$

where  $v_{rel}$  is the relative velocity of the pair, and  $\Delta t$  is the simulation timestep length. The limiting case is where

$$r = v_{rel}\Delta t, \quad (46)$$

leads to a slope of one if the separation is plotted logarithmically versus  $v_{rel}\Delta t$  (Figure 11).

The measured slope is 1.05.

The upper line has a negative slope and corresponds to a one-dimensional collision

frequency limit. The one-dimensional collision frequency is given by

$$\nu = k \frac{\eta_{1D}^2}{v_{rel}}, \quad (47)$$

where  $k$  is a proportionality constant (Owens and Lauck, 2017). The local density of the plasma is  $\eta_{1D} = \frac{1}{r}$ . Solving for the relative velocity where the collision frequency equals 1 yields

$$v_{rel} = \frac{k}{r^2}. \quad (48)$$

This equation leads to a slope of negative two in the logarithmic plot of separation versus  $v_{rel}\Delta t$  (Figure 11). The measured slope is -2.01.

### Reactivity

Figure 12 shows the average fusion reactivity, or average reactive volume per second, from 6 simulation runs of 1000 timesteps, where  $\Delta t = 7.94 \times 10^{-13}$  seconds and kinetic temperatures range from 5 keV to 1000 keV. 10 keV corresponds to 100 million Kelvin. The illustrated simulation results are robust across all kinetic temperatures matching those of Huba (2013) in shape and approximate peak.

The error bars represent 95% confidence intervals assuming a  $t$ -distribution of the sample mean (Larsen and Marx, 2012). For a given kinetic temperature the error bars are calculated using

$$\bar{x} \pm t_{n-1} \frac{sd}{\sqrt{n}}, \quad (49)$$

where  $\bar{x}$  is the sample mean,  $n$  is the number of samples,  $t_{n-1}$  is the value from a Student  $t$ -distribution with  $n-1$  degrees of freedom, and  $sd$  is the standard deviation of the samples.

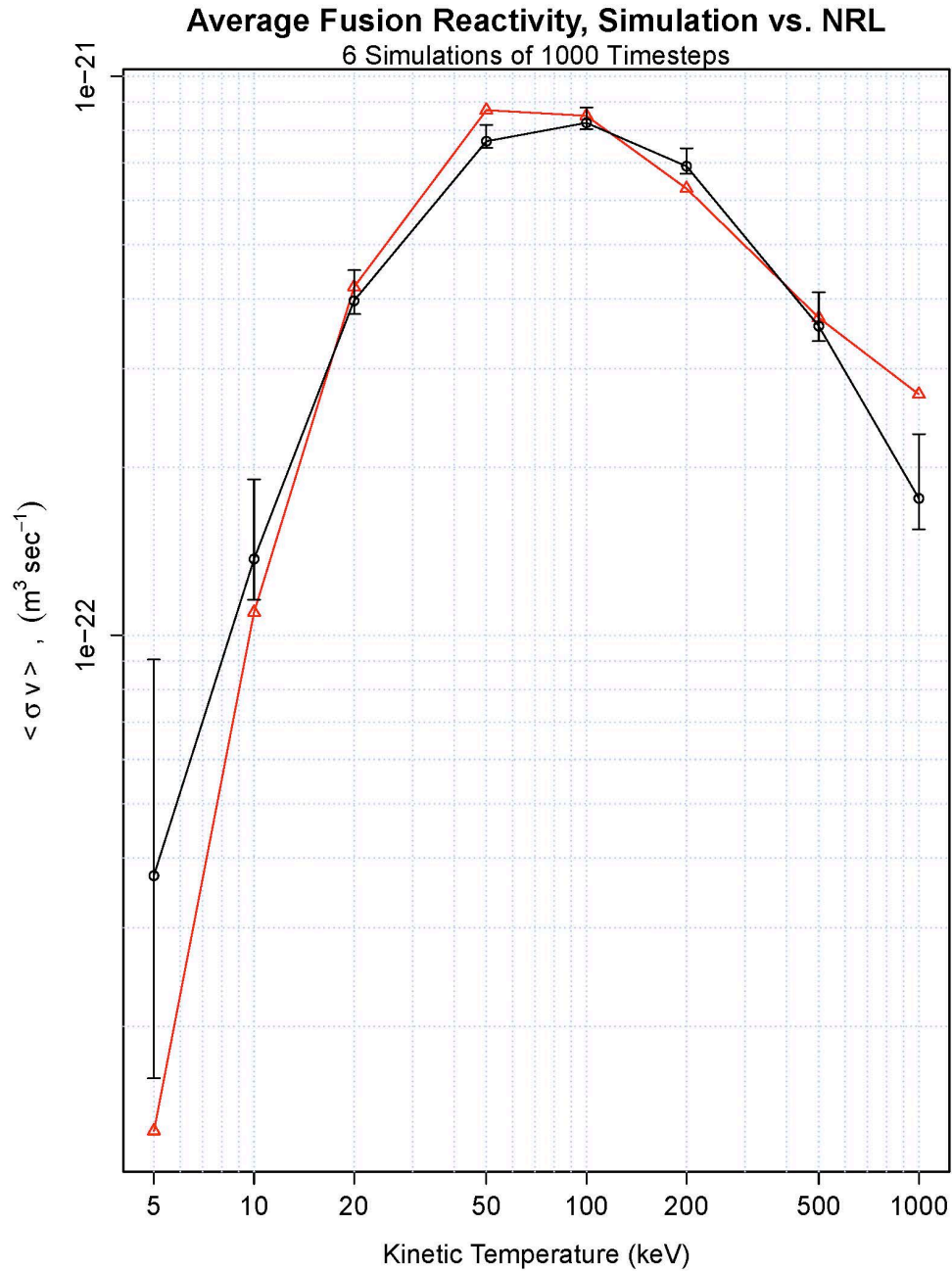


Figure 12: Simulation and Naval Research Laboratory (Huba, 2013) average fusion reactivity from 6 simulations of 1000 timesteps plotted logarithmically. NRL fusion reactivity values are plotted as red triangles. Simulation fusion reactivity values are plotted as black circles. Error bars represent a 95% confidence interval.

Table 1: A sample of simulation results after 500 timesteps. The “Total Collisions” are the sum of the “Fusion” count and the “Not Fusion” count.

<b>keV</b>	<b>Total Collisions</b>	<b>Fusions</b>	<b>Not Fusions</b>
5	4592576	3	4592573
10	3332348	15	3332333
20	2402455	78	2402377
50	1545279	393	1544886
100	1101967	895	1101072
200	781797	1588	780209
500	496998	2261	494737
1000	351376	2693	348683



## DISCUSSION

As can be seen in the Results section, one-dimensional collision and fusion events can be transformed by Equation 37 into a three-dimensional fusion reactivity. The resulting reactivity matches empirical expectations in the case of isotropic plasmas (Figure 12). We expected that only head-on collisions would result in fusion events due to their higher relative kinetic energy, as compared to an overtaking pair of particles. We did not expect to find that the majority of fusion events were caused by overtaking collisions.

The relationship between the separation and relative velocities of fusion pairs is surprising. We do not understand why head-on relative velocity particles have smaller separations while the lower relative velocity pairs have greater separations. This result is counterintuitive and must be explored in further research.

An early concern was whether there would be issues with particles occupying the same space, but these events appear to be rare. As explained previously, in the simulation there are no “safety” checks for this non-physical situation. Instead, particle collisions and the background electric field govern the particle motion and interactions in the plasma. The fact that particles avoid occupying the same space naturally evolves from the model.

In this thesis I have shown that one-dimensional particle interactions can be modeled, simulated, and transformed to accurately predict three-dimensional dynamics in isotropic plasmas. Simulation results match well to experimental plasmas with magnetic fields though the one-dimensional model was developed with an electrostatic assumption.

### Future Work

Future work related to this thesis includes exploration of the bimodal distribution of relative velocities and separation between fusion pairs. Understanding how and why these

distributions occur is critical to further validate the model.

The simulation developed for this thesis ignores electron collisions. The velocity difference between ions and electrons is so great, that to accurately account for electron interactions, the simulation timestep must be on a scale where the ions are essentially stationary. More research is necessary to develop a technique where electron interactions are computed on a GPU, while the CPU computes ion interactions. The FUSION supercomputer was built with this task in mind. This thesis and the existing electron PIC code provide the groundwork to implementing a hybrid GPU-CPU simulation.

Finally, the simulated three-dimensional kinetic energy (Equation 44) may be an upper bound of the kinetic energy for a three-dimensional particle and further research is required to determine if this is an overestimate.

## BIBLIOGRAPHY

- Atzeni, S. and J. Meyer-Ter-Vehn. 2004. *The Physics of Inertial Fusion*. Oxford University Press.
- Duane, B. H. 1972. Fusion cross section theory. Tech. rep., Brookhaven National Laboratory Report BNWL-1685.
- Fitzpatrick, R. 2006. An example 1d pic code. <http://farside.ph.utexas.edu/teaching/329/lectures/node102.html>. Online: accessed 26 July 2016.
- Gamow, G. Z. 1928. Zur quantentheorie des atomkernes. *Zeitschrift für Physik*, **51**(3):204–212.
- Goldston, R. J. and P. H. Rutherford. 2000. *Introduction to Plasma Physics*. Taylor & Francis Group, LLC.
- Griffiths, D. J. 2005. *Introduction to Quantum Mechanics Second Edition*. Pearson Prentice Hall.
- Huba, J. 2013. *Plasma Formulary*. Naval Research Laboratory, Washington, DC.
- Larsen, R. J. and M. L. Marx. 2012. *An Introduction to Mathematical Statistics and Its Applications*. Pearson Education, Inc.
- Owens, K. and T. Lauck. 2017. Predicting three-dimensional collision frequencies from a one-dimensional model. *Unpublished Manuscript*.
- Schroeder, D. V. 2000. *An Introduction to Thermal Physics*. Adison Wesley Longman.
- Serway, R. A., C. J. Moses, and C. A. Moyer. 2005. *Modern Physics*. Brooks/Cole - Thomson Learning.
- Taylor, J. R. 2005. *Classical Mechanics*. University Science Books.
- Thornton, S. T. and A. Rex. 2006. *Modern Physics for Scientists and Engineers*. Thomson Brooks/Cole.
- Waterloo Physics Department. 2010. Nuclear Data. <http://www.science.uwaterloo.ca/~cchieh/cact/nuctek/data.html>. Online: accessed 10 September 2016.

## APPENDIX

### Constants and Calculations

The constants used for all calculations in the simulation are defined in the attached Mathematica output file. Universal constants are defined by Huba (2013) but the mass of Deuterium and Tritium were defined by the University of Waterloo (Waterloo Physics Department, 2010).

The associated Mathematica output file shows how the Lorentz factor and all necessary Maxwell-Boltzman values are calculated. Additionally, the calculations for the tunneling constants,  $E_o$  and  $R_o$  (Equation 27), and the nuclear radius  $r_o$  can be found in the associated Mathematica file.